

INTERNATIONAL SOCIETY FOR SOIL MECHANICS AND GEOTECHNICAL ENGINEERING



This paper was downloaded from the Online Library of the International Society for Soil Mechanics and Geotechnical Engineering (ISSMGE). The library is available here:

<https://www.issmge.org/publications/online-library>

This is an open-access database that archives thousands of papers published under the Auspices of the ISSMGE and maintained by the Innovation and Development Committee of ISSMGE.

Some aspects of measurement of sand thermal conductivity from laboratory tests

Quelques aspects de la mesure de la conductivité thermique du sable à partir d'essais en laboratoire

K. Aljundi (Corresponding author)

A. Vieira, J. R. Maranhã

National Laboratory for Civil Engineering, Lisbon, Portugal

J. Lapa, A. Figueiredo

Aveiro University, Aveiro, Portugal

ABSTRACT: Soil thermal conductivity is a key aspect in the evaluation of the energy efficiency of Shallow Geothermal Energy Systems (SGES). Several factors affect this thermal property, with the water content, the solid particle composition and density being the most relevant. The assessment of soil thermal conductivity can be achieved by distinct methods and procedures. However, several difficulties are associated with many of these methods and a comparison of this property obtained through different methods often results in significantly different estimates. This work presents a study on measured and simulated heat transfer in *Fontainebleau* sand in order to evaluate its thermal conductivity and is part of an ongoing study on soil thermal behaviour. Numerous thermal tests were carried out on samples prepared with different relative densities and water contents with a high accuracy measuring device. Sand thermal conductivity determinations were performed with the line-source based model and with a method based on a back-analysis procedure through numerical modelling of the thermal test taking into account and determining the contact resistance between the thermal probe and the soil.

RÉSUMÉ: La conductivité thermique du sol est un aspect essentiel de l'évaluation de l'efficacité énergétique des systèmes énergétiques géothermiques peu profonds (*Shallow Geothermal Energy Systems* - SGES). Plusieurs facteurs affectent cette propriété thermique, à savoir la structure du sol et sa teneur en eau. L'évaluation de la conductivité thermique du sol peut être réalisée par des méthodes et procédures distinctes. Cependant, plusieurs difficultés sont associées à plusieurs de ces méthodes et une comparaison de cette propriété entre différentes méthodes donne souvent lieu à des estimations très différentes. Ce travail présente une étude sur le transfert de chaleur mesuré et simulé dans le sable de Fontainebleau afin d'évaluer sa conductivité thermique et fait partie d'une étude en cours sur le comportement thermique du sol. Des nombreux tests thermiques ont été effectués sur des échantillons préparés avec différentes densités relatives et teneurs en eau avec un appareil de mesure de haute précision. Les déterminations de la conductivité thermique du sable ont été effectuées avec le modèle basé sur une source linéaire et avec une méthode basée sur une procédure de rétro-analyse par modélisation numérique du test thermique prenant en compte et déterminant la résistance de contact entre la sonde thermique et le sol.

Keywords: thermal conductivity, experimental tests, numerical modelling, back-analysis

1 INTRODUCTION

SGES have been increasingly used revealing significant environmental and social benefits. Compared with other traditional heating and cooling systems, SGES can be considered more sustainable, since they significantly reduce CO₂ emissions from 31% up to 88% (Saner et al. 2010). SGES performance can be affected by many factors such as its location, the local climate conditions, the energy demand of the structure to be conditioned, the ground temperature and the thermal properties of ground where the system is located. Thermal properties can play a major role in assessing the efficiency and designing of SGES, specifically the ground thermal conductivity, λ . Indeed, the thermal conductivity is a dominant factor when compared to other factors, such as the daily temperature amplitude (e.g. Sipio and Berterman, 2017).

Following Fourier's law, thermal conductivity is the coefficient of proportionality between temperature's gradient and the corresponding heat flux, q :

$$q = -\lambda \frac{dT}{dx}. \quad (1)$$

λ can be affected by many different factors, such as moisture content, density, composition and mineral proportions, among others (e.g. Farouki, 1981; Nowamooz et al., 2016). Several studies confirm the importance of the soil degree of saturation, S_r , in the magnitude of thermal conductivity and consequently in soil heat transfer. Soil's thermal conductivity tends to increase with its moisture content, due to the replacement of air, a poor heat conductor by, water which is a much better one. Furthermore, thermal conductivity has a direct correlation with the soil density (e.g. Misra et al., 1995). In fact, increasing the soil density leads to both a decrease of the air fraction in the soil and an increase in the number of contacts between soil particles. Soil state conditions, physical and thermal properties, together with other factors influence thermal conductivity (Maranha and Vieira, 2018). Evaluating thermal con-

ductivity of soils can be carried out by either laboratory or in-situ tests (e.g. Witte et al., 2002). Laboratory measurements on soil samples are known to be cheap and quick, contrary to the field measurements which are more expensive and require more time and effort (Low et al., 2014).

Despite not accounting for site-specific conditions such as the presence of ground water flow and spatial heterogeneity, laboratory measurements allow a greater control of the main variables involved in the test. However, important difficulties are associated with laboratory measurements of λ such as sample disturbance, destructuration and variation of in-situ water content (Vieira et al., 2017).

Thermal conductivity measurements by laboratory methods can be divided into steady-state and transient methods (e.g. Zhao et al., 2016). In steady-state methods, measurements are performed when the temperature in the tested sample does not change with time. Transient methods enable quick measurements of thermal conductivity as they do not need steady-state conditions to be reached. They could be either frequency-domain, as in the pulsed power technique, or time-domain, as in the hot-wire, plane-source or the laser flash methods (Semlyen and Iravani, 1993). The main advantages and disadvantages of both type of methods are referred in Vieira et al. (2017).

This work is focused on the evaluation of the thermal conductivity of *Fontainebleau* sand. It is part of an ongoing research which includes the study of different types of reconstituted and natural soils. The thermal measurements were carried out on transient conditions using a measurement and control unit connected to a thermal probe with temperature transducers (TPSYS02-02). Measurements of the sand conductivity for different relative densities (from minimum to maximum) and different moisture contents (corresponding from dry to fully saturated conditions) were performed. In order to simulate numerically the test results, the conductance between the thermal probe and the soil sample was also determined.

2 EXPERIMENTAL STUDY

2.1 Method theoretical basis

The method used by the measuring equipment to determine thermal conductivity is based on the line-source solution proposed by Carslaw and Jaeger (1959). It relies on the idealization of a radial heat flux from a linear heat source (the hot wire) of infinite length and infinitesimal diameter, and on the temperature rise measurement at a specified distance of the heat source embedded in the tested material. λ can be derived from the temperature change over a specified time interval due to a constant radial heat flux generated by a current of fixed intensity through a resistive wire.

The transient temperature variation can be obtained as a function of time and at a fixed distance from the linear heat source with a constant heat flux rate per unit length, Q . For sufficiently large values of elapsed time, the analytical solution of the governing equations can be simplified resulting in the following relation (e.g. Franco, 2007):

$$\lambda = \frac{Q}{4\pi(T_2 - T_1)} \ln\left(\frac{t_2}{t_1}\right), \quad (2)$$

which enables the evaluation of the thermal conductivity when the temperature rises from T_1 to T_2 , respectively, between instants t_1 and t_2 .

Time instants t_1 and t_2 must be identified post-test as the limits of the time interval where the plot of normalized temperature change $4\pi(T - T_0)/Q$ versus the natural logarithm of time is approximately linear. λ is the inverse of the line slope.

The thermal conductivity measurement system used adopts the procedure described above.

The probe (thermal) needle has a total length of 15 cm, where a heating wire runs along the upper 10 cm. A thermocouple junction for measuring the needle temperature is located at half-length of the heating wire. The measuring method follows ATSM D5334-00 and IEEE Std 442-1981 standards procedures.

However, as noted by Farouki (1981), there are factors in this methodology, that differ from the idealized continuous heat line source conditions, and can be a source of errors, such as the finite length, radius and heat capacity of the probe, as well as the contact resistance between the probe and the medium.

2.2 Equipment description

This system is designed to perform high accuracy measurements of thermal conductivity following the transient method of heat conduction using non-steady-state probes. The range of λ that can be measured is [0.1 and 6] W.m⁻¹.K⁻¹. The system includes the following parts (Figure 1): (1) thermal probes TP02 or TP08; (2) PC with control software connected to control unit; (3) the sample where the probe will be inserted; (4) CR1000 measurement and control unit (MCU) (Hukseflux, 2014).

2.3 Samples preparation

Before performing the thermal measurements, the soil was characterised, determining its granulometric distribution, initial water content, void ratio, maximum and minimum dry densities, ρ_{dmax} and ρ_{dmin} (Table 1).

Table 1. Minimum and maximum dry densities and void ratios

Sample	ρ_{dmin} (kg.m ⁻³)	e_{max}	ρ_{dmax} (kg.m ⁻³)	e_{min}
5118	1440	0.855	1750	0.521

A series of precautions were taken in the samples' preparation before conducting each thermal response test. The choice of the sample dimension, specially its minimum diameter (with the purpose of approaching the line-source condition) and its diameter to height ratio (for approaching the infinite medium condition) are of particular relevance.

In all the cases, a good contact between the soil and the probe should be guaranteed. For undis-

turbed soil specimens ASTM D 5334 – 08 standard indicates a minimum diameter of the sampling recipient containing the soil specimen of 51 mm. On the other hand, the equipment manual refers that the recipient radius should not be less than 15 times the needle probe radius (Hukseflux, 2014). Therefore, for the case of the used thermal probe (TP02), which has a diameter of 1.5mm, the recipients' minimum diameter should not be less than 22.5mm. Thus, to fulfil this condition and to study the possible boundary effect, three diameters were selected in this work, namely: 50mm, 80mm and 100mm.



Figure 1 - Laboratory set-up of TPSYS02-02 system

The height of the recipient is also critical, since it should allow the insertion of the entire needle in the soil sample which in this case implies a length of 200 ± 30 mm of. The recipients were made with a height of nearly 250mm. The soil specimens were prepared for five relative densities D_r (0%, 30%, 45%, 60% and 100%).

Specific techniques were used to achieve the proposed range of D_r values and also to obtain conditions from totally dry to saturated.

To achieve the minimum density of *Fontainebleau* sand, with an almost monogranular distribution, a sand pluviation device was used. Special care was required with the lowest density sample since any movement could lead an increase in density. For higher densities, a selection of an appropriate compaction technique was required. For instance, to achieve densities higher than the minimum (1520, 1560 and 1610 $\text{kg}\cdot\text{m}^{-3}$), the sample was manually compacted in 3 equal layers to the desired density taking care to avoid damaging or crushing the sand particles and changing its grain-size distribution. An almost

homogenous density was obtained with this technique.

For the maximum density, 1750 $\text{kg}\cdot\text{m}^{-3}$, standard ASTM D 4254-00 was followed using a vibratory table. The first series of samples was set-up in totally dry conditions. A sample was prepared for each recipient diameter. Figure 2 shows a dry sample with the thermal probe inserted.



Figure 2- Thermal probe inserted in the sand sample during thermal conductivity measurements

Regarding the partially saturated sand samples, in order to obtain the required water content, w , water was added to the sand and mixed until achieving a homogeneous mixture for the moist sample. Three water contents were tested: 5%, 10% and 15%. For the preparation of the samples the moist sand was placed in the recipient and compacted in 3 layers to the desired density.

During the samples' preparation, for the medium densities, such as 1560 $\text{kg}\cdot\text{m}^{-3}$ and for $w=15\%$, it was very difficult to insert the thermal probe into the soil specimen. Thus, in order to avoid damaging the probe, higher densities with moisture content $w=15\%$ were not executed with this procedure.

For the saturated sand samples, the sand in dry conditions was first prepared to the desired density. Afterwards, the soil sample was placed inside another container which was gradually filled with water. The water level was slowly raised in the soil specimen until it reached the top of the sample. Filter paper was placed at the bottom of the sample to avoid particles erosion. It was observed that the loosest sample ($D_r=0$) settled during the saturation process. This was due to wetting collapse settlement and led to a decrease in

the void ratio from $e=0.855$ to $e=0.782$. This effect was also noted for the second loosest sample where the change was from $e=0.755$ to $e=0.727$. Figure 3 shows some aspects of the saturated sample preparation and of the settlement on the loosest sand.



Figure 3 - Saturated sand sample preparation and sand level changes

After preparing the sand samples with five densities ranging from 1400 to 1750 kg.m^{-3} and different saturation degrees, the samples were re-weighted and their respective densities verified. The thermal probe was afterwards inserted into each sample. Special care was taken to ensure introducing the needle properly and avoid damaging it, particularly for the densest samples.

Each test was identified by the sample water content (dry - d, water content of 5, 10 and 15% - w5, w10 or w15 - or saturated - s), recipient diameter (50, 80 or 100 mm - m1, m2 or m3) and initial density (1440, 1520, 1560, 1610 or 1750 kg.m^{-3} - d144, d152, d156, d161 or d175).

3 RESULTS OF THERMAL CONDUCTIVITY MEASUREMENTS

After inserting the needle, the samples' temperature was registered until it equalized with the room temperature (thermal balance between the sample and the exterior).

The thermal load consisted on the application of a constant heat flux, $q=180.4 \text{ W.m}^{-2}$, for 100s. Various control parameters are displayed and recorded during the test so that its quality and the measures' reliability can be verified. Figure 4

shows a global plot of the measurements. The effect of the samples saturation ratio and density are clearly observed.

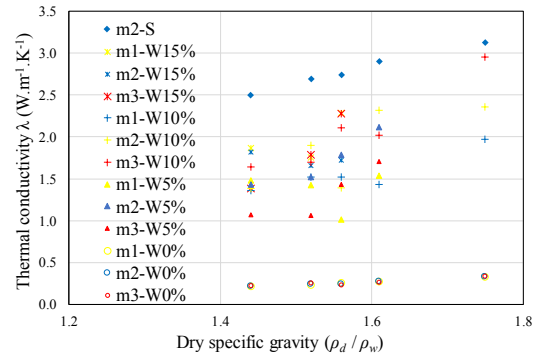


Figure 4 - Thermal conductivity measurements as a function of dry specific gravity (W - water content, m - recipient diameter, S - saturated)

The values of λ ranged from nearly 0.2 to 3.2 $\text{W.m}^{-1}.\text{K}^{-1}$. For the heating time used there was no discernible effect of the sample diameter.

4 BACK-ANALYSIS OF THE THERMAL CONDUCTIVITY TESTS

4.1 Numerical analyses

In order to verify the validity of the experimental procedure used to measure the thermal conductivity that was described above, for some specified tests, the thermal conductivity was determined by means of back-analyses using numerical simulations of the heat transfer process. The finite difference code FLAC2D (Itasca, 2005) was used for that purpose.

The heat flow was assumed as radial implying axisymmetric conditions. The mesh has a single 4 noded quadrilateral element in the vertical direction (the height being irrelevant) by 100 elements in the horizontal direction. The inner boundary coincides with the surface of the measuring needle at $r=0.75\text{mm}$ and the outer boundary is at $r=50\text{mm}$ that is the radius of the modelled samples. The element horizontal thickness increases from 0.1577mm at the inner boundary to 1.12mm at the outer boundary. A constant heat

flux $q=180.4\text{Wm}^{-2}$ was prescribed to the inner boundary and ambient temperature at the outer boundary. At the beginning of the test, the sample was assumed to be in thermal equilibrium with the ambient temperature that was considered as the initial temperature at all the nodes. The top and bottom boundaries are adiabatic. The heat flux was applied for 100s as in the tests and a time step of 0.001s was used. In order to perform the simulation, the soil's heat capacity must be known. It can be computed with sufficient accuracy if the heat capacity of the soil particles is known, which in this case, is that of quartz. The heat capacity per unit mass of the soil was obtained from the mass heat capacities of its constituents as

$$c = \chi_s \frac{\rho_s}{\rho} c_s + \chi_w \frac{\rho_w}{\rho} c_w + \chi_a \frac{\rho_a}{\rho} c_a, \quad (3)$$

which is a weighted arithmetic mean with the respective mass fractions as relative weights. c_s , c_w , and c_a are the specific heat capacities of the solid, water and air phases, $\chi_s=1-n$, $\chi_w = nS_r$ and $\chi_a = n(1 - S_r)$, the soil density is $\rho = \chi_s \rho_s + \chi_w \rho_w + \chi_a \rho_a$ and ρ_s , ρ_w and ρ_a are the corresponding densities.

The following values were used: $c_s=733$, $c_w=4186$ and $c_a=1012 \text{ J.kg}^{-1}.\text{K}^{-1}$. The resulting c values are shown in Table 2. The computed temperature at the inner boundary was compared to the measured needle temperature. 6 tests were selected for the numerical simulations: 3 tests with dry samples at different relative densities, a saturated sample and 2 samples at an intermediate relative density, with $w=5\%$ and $w=10\%$. In principle dry and fully saturated samples provide more reliable measurements because a greater heterogeneity of the moisture distribution in the samples is expected under partially saturated conditions (water movement due to gravity at higher moisture contents and fast change in air relative humidity at the boundaries).

4.2 Numerical results

For all the analysed tests a first numerical calculation of the heat conduction was carried out

assigning to the soil thermal conductivity the value obtained in the corresponding laboratory test. As can be seen in Figure 5, in the case of the simulation of the saturated sample, the rate of temperature increases and the final temperature obtained numerically are much lower than the measured ones. Also even if it was possible to reach the observed final temperature for a much reduced value of λ , the intermediate computed temperatures would be very significantly below the actual ones. This was the case for all the simulations and is an indication of a considerable contact thermal resistance between the needle and the soil. The contact thermal resistance was then simulated by attributing reduced values of thermal conductivity, λ_c , to the very thin element (0.1577mm) at the inner boundary. The values of both λ and λ_c were then adjusted to the laboratory curve simultaneously. As can be seen in Figure 5 the use of this procedure produced quite good adjustments to the time evolution of the measured needle temperature. It also has the benefit of determining the value of the contact thermal resistance between the metal needle and the soil. The contact thermal conductance, h_c , (the inverse of the contact thermal resistance) can be computed from

$$h_c = \lambda_c / \left[r_0 \ln \left(1 + \frac{\Delta x}{r_0} \right) \right], \quad (4)$$

where λ_c is the conductivity of the thin layer that is used to simulate the contact and is obtained from the back analysis, Δx is the thickness of the layer and r_0 is the radius of the needle.

The resulting thermal conductivity estimates were also compared with semi-empirical proposals based on the spatial arrangement of the soil constituents. According to the geometric mean, λ is obtained by

$$\lambda = \lambda_s^{\chi_s} \cdot \lambda_w^{\chi_w} \cdot \lambda_a^{\chi_a}, \quad (5)$$

where λ_s , λ_w λ_a are, respectively, the thermal conductivity of solid, water and air components. Jougnot and Révil (2010) proposed a definition of thermal conductivity by considering glass spheres with diameter of 200 μm :

$$\lambda = \frac{\lambda_f}{f} \left[f \cdot \theta + \frac{1}{2} (1 - \theta) (1 - \theta + \sqrt{(1 - \theta)^2 + 4f\theta}) \right] \quad (6)$$

where $f = n^{\frac{\alpha}{1-\alpha}}$, $\theta = \frac{\lambda_s}{\lambda_f} > 1$, $\lambda_f = S_r^\beta \lambda_w + (1 - S_r^\beta) \lambda_a$, $\alpha=1.7$ and $\beta=1.52$.

The thermal conductivity values obtained from the back-analysed tests (λ_{meth2}) with those obtained from the line source-based solution (λ_{meth1}) as well as the thermal contact conductance (h_c)

are presented in Table 2. In Figure 6 are plotted the evolution of thermal conductivity with saturation degree for the samples with a void ratio of $e=0.712$ as well as the saturated one with $e=0.782$ (it was $e=0.852$ before saturation) for both methods and for equations 5) and 6).

For saturated conditions all values, both the measured and those obtained from the equations are very similar. In dry conditions both measurements and equation 6) values are quite similar, while the geometric mean expression gives a much larger value.

Table 2. Resume numerical back-analysed tests

	e	S_r	c (J.kg ⁻¹ .K ⁻¹)	Dens. (kg.m ⁻³)	T_i (°C)	λ_{meth1} (W.m ⁻¹ .K ⁻¹)	λ_{meth2} (W.m ⁻¹ .K ⁻¹)	λ_c (W.m ⁻¹ .K ⁻¹)	h_c (W.m ⁻² .K ⁻¹)
dm1d144	0.854	0	733	1440	18.965	0.21	0.21	0.040	279
dm1d156	0.712	0	733.1	1560	20.364	0.23	0.23	0.038	265
dm1d175	0.526	0	733	1750	18.851	0.31	0.24	0.039	272
w5m1d156	0.712	0.188	898.5	1632	18.830	1.14	0.80	0.050	349
w10sm1d156	0.712	0.375	1047.7	1710	20.684	1.70	1.94	0.039	265
sm1d144	0.782	0.97	1517.5	1932	19.925	2.50	2.60	0.035	244

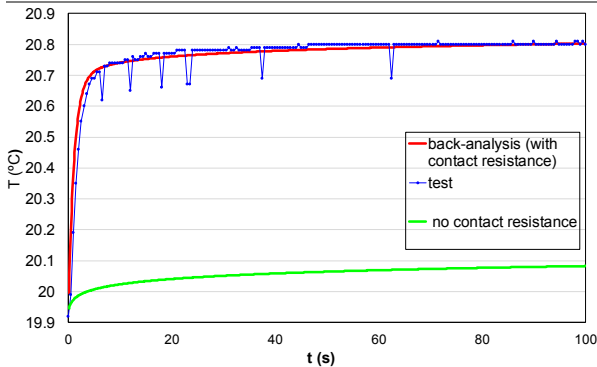


Figure 5 - Thermal test sm1d144 experimental curve. Numerical modelling: line-source model value and back-analysis.

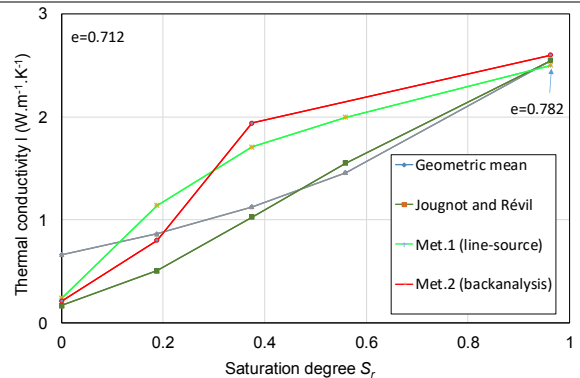


Figure 6 - Evolution of thermal test with the degree of saturation (experimental methods and semi-empirical relations).

For partially saturated conditions there is a significant difference between both measurement methods and between the measurements and the empirical equations. This dispersion of values is probably due to the heterogeneous moisture distribution in the sample which could not be avoided with the used experimental procedure.

The thermal conductance obtained by the back-analysis gave values between 244 and 349 W.m⁻².K⁻¹, which indicates a high contact resistance between both materials (sand and metal).

5 FINAL REMARKS

In this work it was presented a large set of experimental measurements of thermal conductivity in *Fontainebleau* sand for different relative densities and degrees of saturation. Thermal conductivity exhibited a large range of variation mainly due to S_r variation and to a much less extent to D_r . With a back-analyses procedure assuming a different thermal conductivity in the

contact between the soil sample and the needle probe the thermal tests were fully reproduced and the contact thermal conductance obtained. The values indicated a high contact resistance between both materials. Very close thermal conductivity estimates were obtained with both experimental methods. In saturated and dry conditions this agreement was extended to semi-empirical correlations, however under partial saturation this agreement was not attained which might be due to heterogeneity of the moisture content in the sample volume.

6 ACKNOWLEDGEMENTS

The authors acknowledge the support provided by the FCT (Portuguese Foundation for Science and Technology), under the Project SUCCESS (PTDC/ECM-GEO/0728/2014).

7 REFERENCES

- ASTM D5334-00. Standard Test Method for Determination of Thermal Conductivity of Soil and Soft Rock by Thermal Needle Probe Procedure, ASTM International, West Conshohocken, PA, 2000.
- Carslaw, H. S., Jaeger, J. C. 1959. *Conduction of heat in solids*, Oxford Science Publications, Oxford.
- Farouki, O.T. 1981. *Thermal Properties of Soils*. CRREL-MONO-81-1; U.S. Army Corps of Engineers, Research and Engineering Laboratory: Hanover, NH, USA.
- Franco, A. 2007. An apparatus for the routine measurement of thermal conductivity of materials for building application based on a transient hot-wire method. *Applied Thermal Engineering*, **27**, 2495–2504.
- Hukseflux, 2014: TPSYS02 Thermal conductivity measurement system user manual.
- Jougnot, D., Révil, A. 2010. Thermal conductivity of unsaturated clay-rocks. *Hydrology and Earth System Sciences*, **14**, 91-98.
- Low, J., Loveridge, F., et al., A comparison of laboratory and in situ methods to determine soil thermal conductivity for energy foundations and other ground heat exchanger applications. *Acta Geotechnica*, **10**(2), 209-218.
- IEEE Std 442-1981 – IEEE Guide for Soil Thermal Resistivity Measurements, 1-16.
- ITASCA (2005). *Fast Lagrangean Analysis of Continua*, Version 5.0. User’s Manual, Itasca Consulting Group, Minneapolis, Minnesota.
- Maranha, J.R.,Vieira, A. 2018. Stress dependency of the thermal conductivity of a regular arrangement of spheres in a vacuum. *Proc. NUMGE IX*, Francis & Taylor, Porto, Portugal, 737-741.
- Misra, A., et al., 1995. A theoretical model of the thermal conductivity of idealized soil. *HVAC&R Research*, **1**(1), 81-96.
- Nowamooz, H., Nikoosokhan, S., et al., 2016. Seasonal thermal energy storage in shallow geothermal systems: Thermal equilibrium stage, *E3S Web of Conferences* **9**, 07003.
- Saner, D., et al., 2010. Is it only CO₂ that matters? A life cycle perspective on shallow geothermal systems, *Renewable and Sustainable Energy Reviews* **14**(7), 1798-1813.
- Semlyen, A., Irvani, M. 1993. Frequency domain modelling of external systems in an electro-magnetic transients program, *IEEE Transactions on Power Systems* **8**(2), 527-533.
- Sipio, E.D., Bertermann, D. 2017. Factors influencing the thermal efficiency of horizontal ground heat exchangers. *Energies* **10**(11).
- Vieira, A., et al. 2017. Characterisation of ground thermal and thermo-mechanical behaviour for shallow geothermal energy applications. *Energies* **10**(2), 1-53.
- Witte, H.J.L., G.J. van Gelder, J.D. Spitler. 2002. In-situ measurement of ground thermal conductivity: The Dutch perspective, *ASHRAE Transactions* **108**(1), 263-272.
- Zhao, D., Qian, X., et al., 2016. Measurement techniques for thermal conductivity and interfacial thermal conductance of bulk and thin film materials, *Journal of Electronic Packaging* **138**(4), 1-19.